AIAA JOURNAL
Vol. 32, No. 1, January 1994

Drag and Lift in Nonadiabatic Transonic Flow

Günter H. Schnerr* and Ulrich Dohrmann†
University of Karlsruhe, Karlsruhe, Germany

Transonic flows with heat addition over airfoils have been calculated for different angles of attack. The fluid is a mixture of an inert carrier gas and a small amount of a condensible vapor. For the phase change process coupled to the flow, two limiting cases are investigated: nonequilibrium condensation after significant supersaturation and homogeneous nucleation and equilibrium condensation. Numerical calculations based on the Euler equations are linked with either the classical nucleation theory coupled with microscopic or macroscopic droplet growth laws or an equilibrium process. An improved explicit time-dependent diabatic finite volume method is developed and applied to calculate stationary flows. Reservoir conditions of pressure, temperature, and vapor content are varied to simulate internal flows in transonic wind tunnels, turbomachinery, and atmospheric flight at low altitudes. The pressure drag and the lift may increase or decrease. Homogeneous condensation in internal flows produces a maximum decrease of the pressure drag of about 60% and a maximum lift decrease of 35%. Nonequilibrium phase transition of the vapor content in atmospheric flight decreases the lift about 10%, whereas the drag remains nearly constant. With the assumption of the more realistic equilibrium condensation process in atmospheric flight, the lift changes inversely; it increases about 30%, but the pressure drag increases more than 200%. Nonequilibrium and equilibrium condensation in transonic flow are quite easy to distinguish by the position and the extension of the normal shock. The equilibrium process enlarges the supersonic area remarkably, whereas it reduces in size when the vapor condenses not in equilibrium, i.e., gasdynamic phenomena may be used as a tool for the identification of the nature of the actual phase transition process.

Nomenclature

c	= airfoil chord length
c_D	= pressure drag coefficient
c_L	= lift coefficient
c_p	= pressure coefficient
G	= Gibb's free enthalpy
g	= mass fraction of condensate
h	= enthalpy
J	= nucleation rate
k	= Boltzmann constant
L	= latent heat
$M_{f,\infty}$	= frozen freestream Mach number
M_∞	= freestream Mach number
m	= mass per molecule, water
p	= static pressure
$p_{s,r}$	= saturation pressure of droplet with radius r
R_v	= specific gas constant of water vapor
r	= droplet radius
s	= supersaturation ratio
T	= temperature
t	= time
x	= Cartesian coordinate; mixing ratio
y	= Cartesian coordinate
α	= condensation coefficient, angle of attack
Δ	= difference
ρ	= density
σ_∞	= surface tension of a plane surface
Φ	= relative humidity

Subscripts

c	= condensate condensation onset
f	= frozen
q	= heat addition
s	= saturation
v	= vapor
0	= stagnation condition
1	= before heat addition
∞	= freestream; plane surface
*	= values at $M = 1$; values of critical nucleus

Presented as Paper 91-1716 at the AIAA 22nd Fluid Dynamics, Plasma Dynamics, and Lasers Conference, Honolulu, HI, June 24–26, 1991; received Feb. 10, 1992; revision received June 1, 1993; accepted for publication June 27, 1993.

*Professor, Doctor of Engineering Sciences, Institut für Strömungslehre und Strömungsmaschinen, Department of Mechanical Engineering. Senior Member AIAA.

†Doctor of Engineering Sciences, Institut für Strömungslehre und Strömungsmaschinen, Department of Mechanical Engineering.

Introduction

IN transonic and supersonic expansion flows of pure vapors or vapor/carrier gas mixtures, the fluid may undergo a phase change by condensation as observed in steam turbines, cryogenic turbomachinery, shock tubes, and wind tunnels and around airplane wing sections in atmospheric flight. Then the latent heat release corresponds to a high concentration of internal heat sources that causes significant variations in aerodynamic characteristics of lift and drag, even in the most critical state near Mach number unity. In adiabatic transonic flows small parameter variations are already known to alter the flow considerably. For heat addition or removal by condensation or evaporation, the same sensitivity is achieved, even for condensate mass fractions of only a few percent.

In expansions that are not too fast, the number of droplets is controlled by present foreign nuclei, dust particles, aerosols, or ions. These heterogeneous processes can develop, either near equilibrium or in a supersaturated state, whereas fully equilibrium condensation leads to the upper limit for the possible condensate mass fraction. High cooling rates up to $-1°C/\mu s$ are required for nucleation in the pure vapor phase and for the production of droplet concentrations typically 5–10 orders higher than those in heterogeneous condensation. Assuming the two models of equilibrium and homogeneous condensation, transonic flows over a NACA 0012 airfoil that reveal the behavior of two phase flows in turbomachinery and aerodynamics have been investigated numerically.

A more detailed description of the condensation models used herein can be found in the comprehensive monographs of Wegener and Mack,[1] Wegener,[2] and Abraham.[3] Condensation phenomena in transonic flow around airfoils were first reported by Head,[4] Schmidt,[5] and Hiller and Meier.[6] A summary of the visualization of homogeneously condensing flows over airfoils can be found in Schnerr,[7] including empirical relationships for the condensation

onset. Well-established similarity laws for the condensation onset or more generally for heat addition in transonic flows are formulated by Zierep and Lin[8] and Zierep.[9,10] Cryogenic wind-tunnel experiments dealing with condensation effects around airfoils in transonic flows of nitrogen are presented by Hall,[11,12] Kilgore,[13] and Wegener.[14] Many details of humidity effects on aerodynamic characteristics of a NASA supercritical airplane model are investigated by Jordan.[15] A stimulating summary of visualizations of natural condensation effects in airplane flowfields and numerical calculations are presented by Campbell et al.[16] Appropriate numerical results for condensing transonic flows over airfoils are published by Robinson et al.,[17] Schnerr and Dohrmann,[18,19] and Dohrmann.[20] The corresponding wet steam flow problem in turbine cascades, including the transition to unsteady flow and shock oscillations, has been investigated by Moheban and Young,[21] Guha and Young,[22] and Young and Guha.[23]

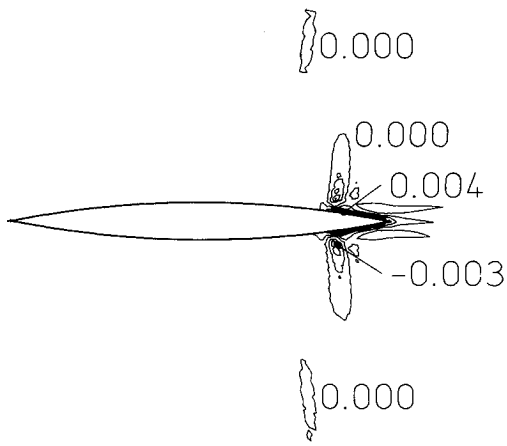

Fig. 1 Contours of constant values $[h_{01} - (h_0 - gL)]/h_{01}$, diabatic flow, $q/c_p T_{01} \approx 0.1$, circular arc airfoil, $M_{f,\infty} = 0.87$.

Theory

The equations for mass, momentum, and energy are used in conservation form:

$$\frac{\partial U}{\partial t} + \frac{\partial F}{\partial x} + \frac{\partial G}{\partial y} = Q \tag{1}$$

In Eq. (1) the source term Q represents the latent heat release of the phase change process. Here U is the vector of the dependent variables, and F and G are the conservative flux vectors. For a description of the homogeneous condensation, we introduce the classical nucleation theory of Volmer and the molecular droplet growth model of Hertz-Knudsen:

$$J = \sqrt{\frac{2}{\pi}\sigma_\infty}\, m^{-3/2} \frac{\rho_v^2}{\rho_c} \exp\left(-\frac{\Delta G^*}{kT}\right)$$

$$\Delta G^* = \frac{16}{3}\pi \left[\frac{m}{\rho_c \ell_n(s)\, kT}\right]^2 \sigma_\infty^3 \tag{2}$$

$$\frac{dr}{dt} = \frac{\alpha}{\rho_c} \frac{p_v - p_{s,r}}{\sqrt{2\pi R_v T}} \tag{3}$$

where ΔG^* is the Gibb's free enthalpy for the formation of a nucleus of the critical size. For equilibrium condensation, the pressure and temperature of the condensing component are coupled by the saturated vapor pressure curve. Our two-dimensional, diabatic, finite volume method is explicit in calculating both the dependent variables and the condensate mass fraction dg/dt. This method is time dependent and is developed to calculate stationary flows. For determination of the total energy per unit mass at the cell boundaries, several approximations for the Riemann solver have been tested. Only the most appropriate version that produces a minimum of nonphysical entropy and enthalpy is used for the calculation of the results presented in this paper. Figure 1 shows the

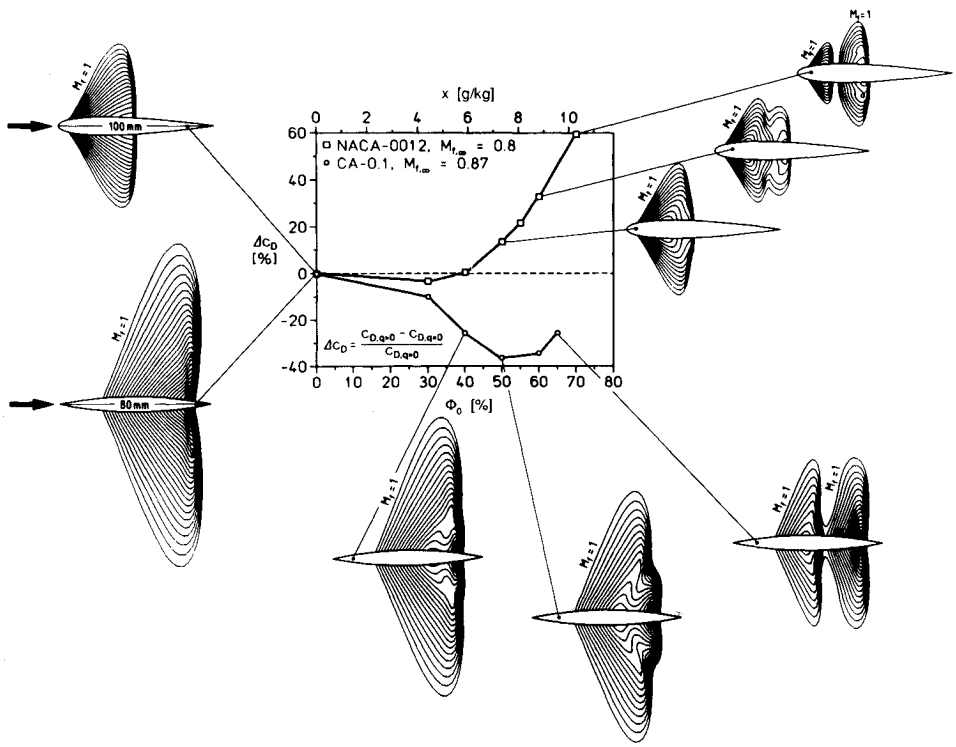

Fig. 2 Pressure drag increase and decrease in homogeneously condensing transonic flows without angle of attack; NACA 0012, $c = 100$ mm, circular arc airfoil CA-0.1, $c = 80$ mm; indraft wind tunnel, moist air, $T_{01} = 293.15$ K, $p_{01} = 1$ bar, supersonic iso-Mach lines ($\Delta M_f = 0.015$).

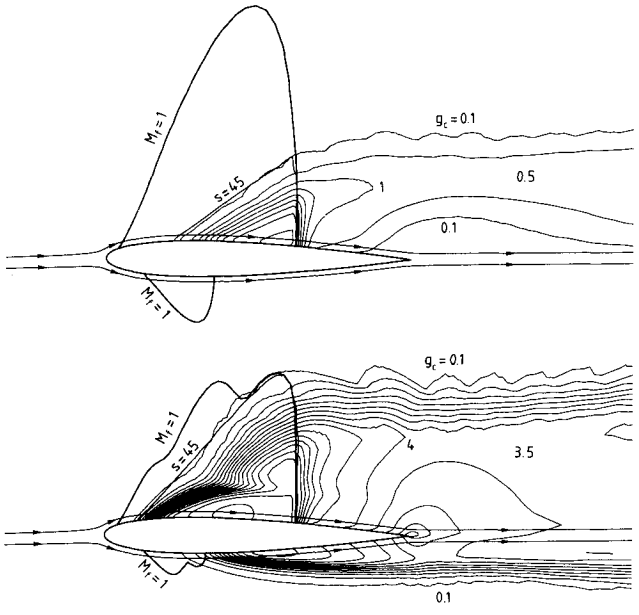

Fig. 3 Contours of constant condensate mass fraction g(g/kg) (Δg = 0.5 g/kg) and constant supersaturation s; NACA 0012, $M_{f,\infty}$ = 0.8, α = 1.25 deg; top—Φ_0 = 30%, bottom—Φ_0 = 70%, IWT.

numerical error of the total enthalpy for the transonic flow around a circular arc airfoil at a freestream Mach number $M_{f,\infty} = 0.87$ and a relative humidity of the water vapor of $\Phi_0 = 50\%$ ($x = 7.34$ g/kg, $T_{01} = 293.15$ K). Plotted are the contours of $[h_{01} - (h_0 - gL)]/h_{01}$ = const, which should be zero everywhere. The remaining nonzero values are caused by numerical dissipation near the normal shocks. More details of the equations and the numerical method are already given by Schnerr and Dohrmann[18] and Dohrmann.[20]

Results

A. Indraft Wind Tunnel

1. Nonlifting Flow, Homogeneous Condensation

We start discussing results for homogeneous condensation in a water vapor/carrier gas mixture (moist air) under reservoir conditions typical for indraft wind tunnels (IWT), i.e., $T_{01} = 293.15$ K, $p_{01} = 1$ bar, $\Phi_0 \cong 30$–70%, and $c = 100$ mm. A summary of nonlifting flows with varying relative humidity over two airfoils, NACA 0012 and a circular arc profile with 10% thickness (CA-0.1), is given in Fig. 2. The maximum amount of heat added increases from left to right. Simultaneously the supersonic onset Mach number, i.e., the Mach number where essentially condensation begins, decreases toward unity. This produces remarkable variations of the static pressure distribution and of the shape of the local supersonic areas. As known from Laval nozzle flows, supercritical heat addition creates additional normal shocks at both airfoils just behind the onset of condensation; that can herein be observed by the formation of a stationary double shock system. Note that the trend in Δc_D with increasing heat addition can be quite different for different configurations and freestream Mach numbers as indicated in Fig. 2. The cooling rate $-dT/dt$ (°C/μs) over the airfoil, which is given by the geometry for constant reservoir conditions, and the extent of the supersonic region are the two primary factors that determine the effect of homogeneous condensation of the flow.

2. Lifting Flow, Homogeneous Condensation

Figure 3 shows the calculated contours of constant mass fraction for diabatic flows over an inclined NACA 0012 airfoil ($M_{f,\infty}$ = 0.8, α = 1.25 deg). Under the assumption that no condensation takes place and for the same freestream conditions, a selected supersaturation contour ($s = 45$) is plotted. Low relative humidities (Φ_0 = 30%) restrict homogeneous nucleation substantially to the supersonic flow at the suction side. We recognize a maximum supersaturation at the condensation onset near the airfoil between 40 and 50. The resulting maximum nucleation rates are of the order $J \approx 10^{22}$–10^{24} m^{-3}s^{-1}. For Φ_0 = 70%, the nucleation process develops at the pressure side as well and yields additional subsonic heat addition, to be recognized by the expansion at the pressure side downstream of the small supersonic area. However, the predominating effect of high relative humidities is the compression at the suction side (Fig. 4). For mixing ratios x below 14 g/kg the normalized heat addition q/c_pT_{01} is less than 10%. In this range the maximum reduction of the pressure drag for an inclined NACA 0012 profile (α = 1.25 deg) is about 25% (Fig. 5). In tendency this is just the opposite behavior of the flow without inclination (Fig. 2). Simultaneously the lift decreases up to 35% (Fig. 6). This results from the compression at the suction side due to condensation. A characteristic maximum develops in drag and lift reduction for a relative humidity of about 50–60%. Here the upper normal shock moves approximately 7% of the chord length, and the shock position reaches its minimum distance from the tip of the airfoil. For higher values of Φ_0 the diabatic compression is partially compensated by a shift of the shock toward the trailing edge, which increases Δc_D and Δc_L relative to their minimum.

B. Atmospheric Flight

1. Homogeneous Condensation

We proceed on the assumption of pure homogeneous nucleation and assume a chord length of c = 1500 mm and freestream condi-

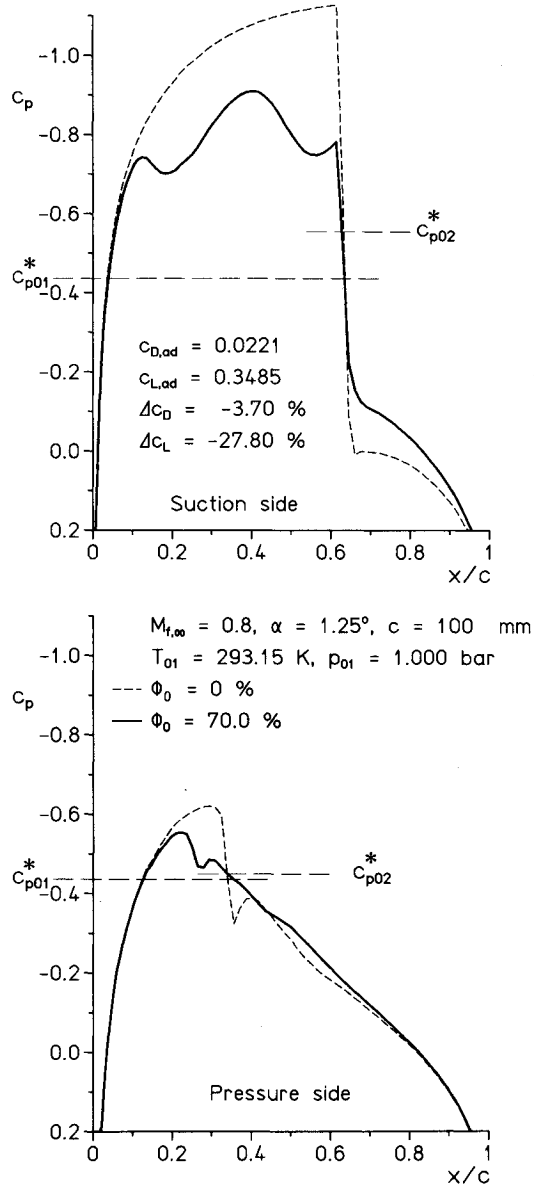

Fig. 4 Pressure coefficient, NACA 0012, diabatic flow, $M_{f,\infty}$ = 0.8, α = 1.25 deg; Φ_0 = 70%, IWT.

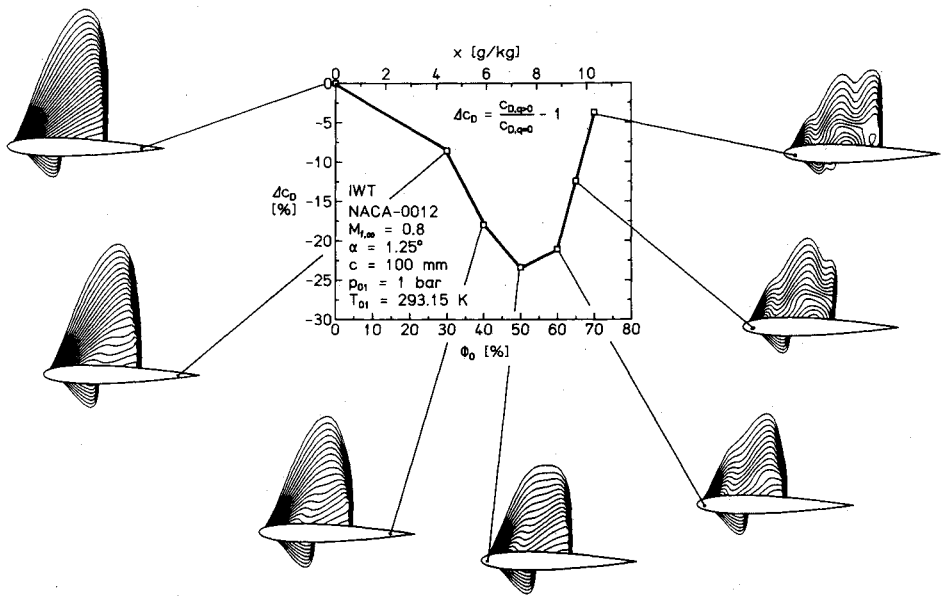

Fig. 5 Pressure drag decrease in homogeneously condensing flow over an inclined NACA 0012 airfoil; indraft wind tunnel, moist air, supersonic iso-Mach lines ($\Delta M_f = 0.015$).

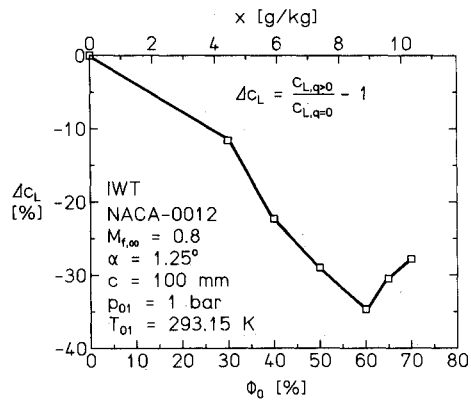

Fig. 6 Lift decrease in homogeneously condensing flow over a NACA 0012; moist air.

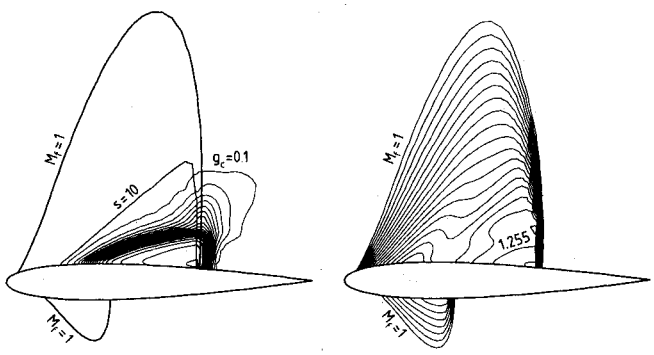

Fig. 7 Atmospheric flight, homogeneous nucleation, NACA 0012, c = 1500 mm, $M_{f,\infty}$ = 0.8, α = 1.25 deg; Φ_∞ = 95%, T_∞ = 293.15 K, p_∞ = 1 bar, left—constant condensate mass fraction contours (Δg = 0.5 g/kg) and contours of constant supersaturation s, right—supersonic iso-Mach lines ($\Delta M_f = 0.015$).

tions (Φ_∞ = 95%, T_∞ = 293.15 K, p_∞ = 1 bar) roughly corresponding to atmospheric flight simulations at low altitudes. Now the maximum supersaturation at the condensation onset is much lower than for IWT flow conditions and for angles of attack between 1.25 and 2.5 deg approximately constant between 10 and 15 (Figs. 7 and 8). Figure 9 shows the Mach number distribution, the condensate mass fraction g/g_{max}, and the nucleation rate J along the stagnation streamline at the suction side of the inclined NACA

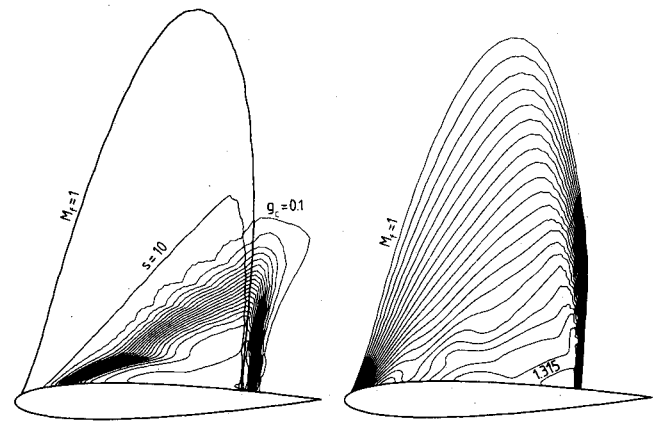

Fig. 8 Atmospheric flight, homogeneous nucleation, NACA 0012, c = 1500 mm, $M_{f,\infty}$ = 0.8, α = 2.5 deg; Φ_∞ = 95%, T_∞ = 293.15 K, p_∞ = 1 bar, left—constant condensate mass fraction contours (Δg = 0.5 g/kg) and contours of constant supersaturation s, right—supersonic iso-Mach lines ($\Delta M_f = 0.015$).

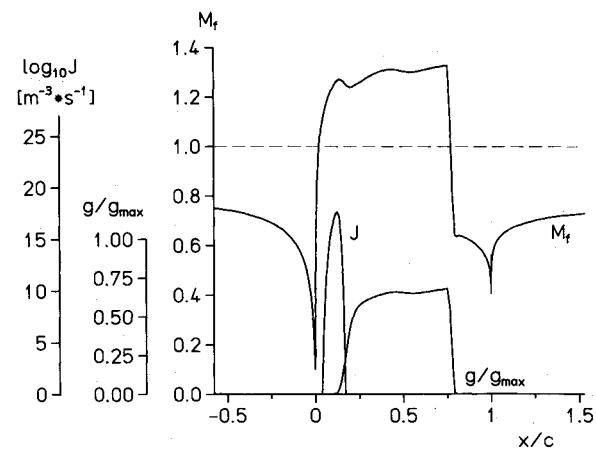

Fig. 9 Frozen Mach number M_f, nucleation rate J, condensate mass fraction g/g_{max} at the suction side of a NACA 0012, $M_{f,\infty}$ = 0.8, α = 2.5 deg (atmospheric flight, see Fig. 8).

0012 airfoil. The substantial decrease of the cooling rate by the greater chord length and the relative humidity (the relevant stagnation value is only 19.1%) reduce the maximum nucleation rate

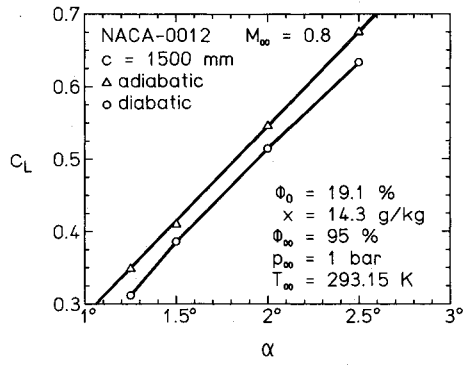

Fig. 10 Lift decrease in atmospheric flight, homogenous nucleation.

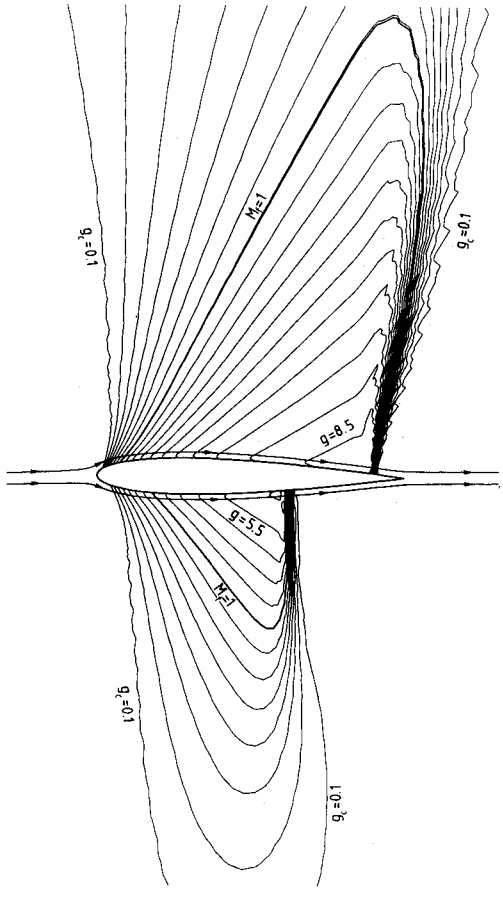

Fig. 11 Equilibrium condensation in atmospheric flight, contours of constant condensate mass fraction g(g/kg) (Δg = 0.5 g/kg); NACA 0012, c = 1500 mm, $M_{f,\infty}$ = 0.8, α = 1.25 deg; Φ_∞ = 95%, (see Fig. 7).

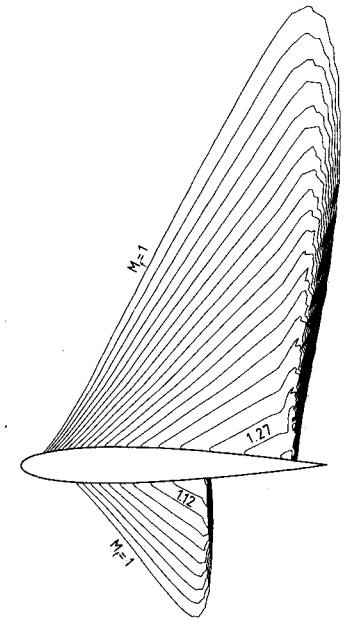

Fig. 12 Equilibrium condensation in atmospheric flight, NACA 0012, c = 1500 mm, $M_{f,\infty}$ = 0.8, α = 1.25 deg; Φ_∞ = 95%, supersonic iso-Mach lines ΔM_f=0.015.

Table 1 Variation of freestream conditions, atmospheric flight, homogeneous nucleation; NACA 0012, c = 1500 mm, $M_{f,\infty}$ = 0.8, α = 1.25 deg

p_∞, bar	T_∞, K	J_{max}, $m^{-3}s^{-1}$	$M_{f,c}$	Δc_D	Δc_L
1	293.15	0.84×10^{17}	1.247	–0.9	–10.5
0.834	293.15	0.72×10^{17}	1.246	–0.3	–10.4
0.500	293.15	0.53×10^{17}	1.243	–0.6	–11.9
0.705	283.15	0.25×10^{18}	1.274	–2.0	–9.4
0.587	273.90	0.77×10^{18}	1.285	–2.8	–8.8

Table 2 Variation of lift and drag in diabatic flow under different test conditions, $q/c_pT_{01} \approx$ const < 0.1, NACA 0012, $M_{f,\infty}$ = 0.8

	Indraft wind tunnel		Atmospheric flight	Cryogenic wind tunnel
Fluid	Moist air	Moist air	Moist air	N_2
Angle of attack, deg	0	1.25	1.25	1.25
Chord length, mm	100	100	1500	100
p_{01}, bar	1	1	1.524	3.604
T_{01}, K	293.15	293.15	330.7	91.10
Φ_0, %	60	60	19.1	91.7
Δc_D, %	+32.9	–21.0	–0.9	–19.5
Δc_L, %	——	–34.7	–10.5	–36.7

more than 5 orders of magnitude in contrast to the flow under conditions typical for indraft wind tunnels. Because of the unsaturated freestream, all droplets evaporate suddenly by the compression over the normal shock. The Mach number contours at the suction side and Fig. 9 indicate a weak supersonic compression, responsible for the lift reduction up to about 12% (Fig. 10). Varying the freestream pressure at constant temperature essentially doesn't affect the maximum nucleation rate and condensation onset Mach number (Table 1). Pressure and temperature combinations in the limits of our investigation that are more representative for higher altitudes do not change the qualitative effects and yield quantitatively the same lift decrease.

Table 2 summarizes the drag and lift variation under different test conditions, indraft wind tunnel, cryogenic wind tunnel, and atmospheric flight, for the same NACA 0012 airfoil and for approximately the same maximum amount of heat addition q/c_pT_{01} < 0.1. Homogeneous condensation in cryogenic and indraft wind tunnels produces quantitatively the same decrease of drag and lift. At zero angle of attack the drag varies in the opposite direction; with inclination the lift decreases without exception.

2. Equilibrium Condensation

In atmospheric flight and the same freestream conditions as before the vapor becomes saturated at a Mach number of 0.834, i.e., the equilibrium condensation process begins already in subsonic flow. The heat addition proceeds continuously over the sonic lines at the pressure and suction side of the airfoil as shown by the contours of constant mass fraction in Fig. 11. However, approximately the same maximum amount of condensate drops out in the equilibrium phase change process as in homogeneously condensing flows of our previous examples after substantial supersaturation. Different are the onset Mach numbers, subsonic for equilib-

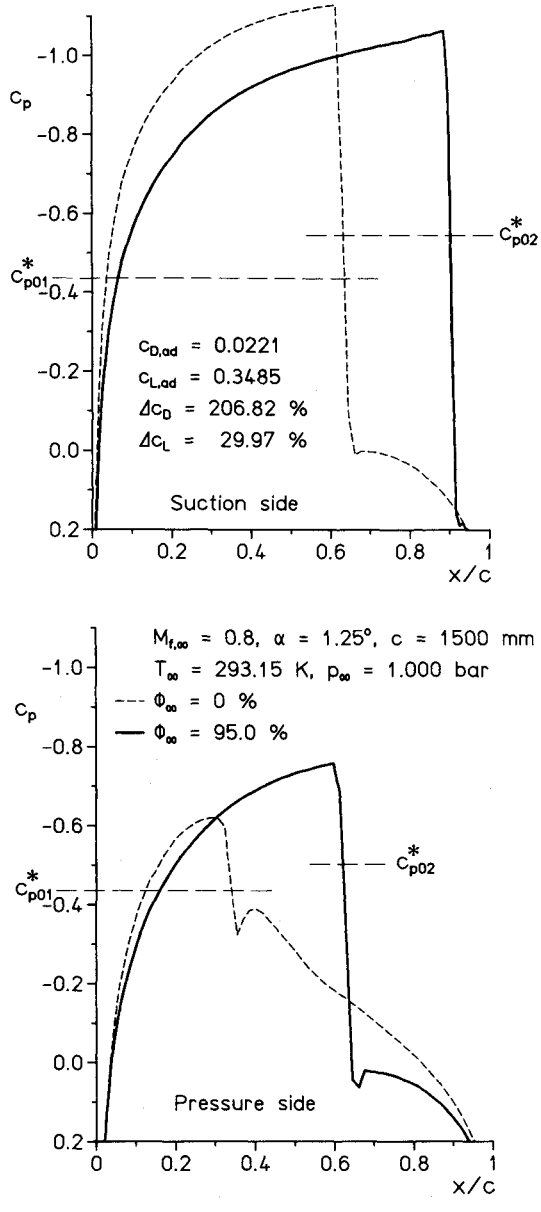

Fig. 13 Equilibrium condensation in atmospheric flight, pressure coefficient, NACA 0012, $M_{f,\infty} = 0.8$, $\alpha = 1.25$ deg.

rium condensation, supersonic for the homogeneous phase change process. The area of heat addition is significantly enlarged, and as a consequence, the gradient of the supply becomes weaker in the equilibrium process than for homogeneous condensation. The iso-Mach lines (Fig. 12) demonstrate important differences to the related diabatic nonequilibrium flow of Fig. 7. Again the different variation of the Mach number contours shown in Figs. 7 and 12 follows only from the actual nature of the phase transition. Figure 13 shows a comparison of the pressure coefficients between the case of $\Phi_\infty = 95\%$ and the related adiabatic flow at the upper and lower surface. Here the heat addition moves the upper shock toward the trailing edge, forming an extended local supersonic area at the pressure side. Overall the lift increases about 30%, but the drag increases substantially more than 200%.

In flows around airfoil wing sections in the atmosphere at pressures and temperatures comparable to those given earlier we expect a mixed heterogeneous/homogeneous phase change process. Numerical investigations and photographs of condensation phenomena by natural light scattering around airplanes in atmospheric flight indicate droplet formation throughout near the equilibrium state (Ludwig[24] and Campbell et al.[16]). The most spectacular pictures of Ludwig present an F-14 during maneuver, flying at $M_\infty = 0.89$ and an altitude of about 300 ft. One picture shows extended condensing areas at the pressure and suction side of the wings. This observation agrees with the tendency shown in Fig. 11 and is clearly impossible in homogeneously condensing flows over inclined airfoils. On the other hand, the typical supersaturation values make homogeneous nucleation possible. As in experiments of Buckle and Pouring,[25] heterogeneous particles tend to diminish the characteristic sudden onset after substantial homogeneous nucleation, and both processes—heterogeneous and homogeneous condensation—proceed at the same time. Further interesting aspects are the overall changes of the cooling rates, corresponding to the gradients of c_p, during equilibrium condensation (Fig. 13); there is a significant decrease at the suction side and the predominating increase at the pressure side.

Conclusions

Numerical calculations demonstrate substantial variations in aerodynamics if heat is added in transonic flows over airfoils either by homogeneous or equilibrium condensation. The pressure drag may increase or decrease for the same amount of heat addition. In equilibrium condensation an increase of lift is possible, but at the same time the drag increases essentially. Comparing both phase change processes in modeling atmospheric flight at low altitudes indicates the necessity for the investigation of the interaction between heterogeneous and homogeneous condensation. However, in accordance with Campbell et al., we expect the predominating phase change in atmospheric flight to develop near equilibrium. Our equilibrium flow calculation reveals the possibility of substantial quantitative effects. In viscous flow we don't expect a different tendency (Schnerr et al.[26] and Schnerr and Li[27]).

This investigation presumes the ideal gas equation for both the vapor phase and the carrier gas. Extending this research to retrograde media leads to the inversion of several gasdynamic effects (Thompson,[28] Cramer,[29] and Cramer and Kluwick[30]). For instance, isentropic compression of a retrograde fluid may lead to condensation and vice versa. Similar results as for our ideal gas calculations are unknown and will be an interesting field for further investigations and technical applications, e.g., for internal transonic flows in organic Rankine cycles (ORC).

Acknowledgments

This work was partially supported by the Deutsche Forschungsgemeinschaft (DFG Contract Zi 18/31) and the Klein, Schanzlin & Becker Stiftung (KSB Contract 1128).

References

[1]Wegener, P. P., and Mack, L. M., "Condensation in Supersonic and Hypersonic Wind Tunnels," *Advances in Applied Mechanics*, edited by H. L. Dryden and T. Kármán, Vol. 5, Academic, 1958, pp. 307–447.

[2]Wegener, P. P., "Gasdynamics of Expansion Flows with Condensation, and Homogeneous Nucleation of Water Vapor," *Nonequilibrium Flows*, Gasdynamics Series of Monographs, edited by P. P. Wegener, Pt. 1, Marcel Dekker, New York, 1969, pp. 163–243.

[3]Abraham, F. F., *Homogeneous Nucleation Theory*, Academic, New York, 1974.

[4]Head, R., "Investigation in Spontaneous Condensation Phenomena," Ph.D. Thesis, California Inst. of Technology, Pasadena, CA, 1949.

[5]Schmidt, B., "Schallnahe Profilumströmungen mit Kondensation," *Acta Mechanica*, Vol. 2, No. 2, 1966, pp. 194–208.

[6]Hiller, W. J., and Meier, G. E. A., "Grenzschichteffekte bei der transsonischen Umströmung eines symmetrischen Profils," MPI Göttingen, Rept. 9, 1977.

[7]Schnerr, G. H., "Homogene Kondensation in stationären transsonischen Strömungen durch Lavaldüsen und um Profile," Habilitationsschrift, Universität Karsruhe, Fakultät für Maschinenbau, Karlsruhe, Germany, 1986.

[8]Zierep, J., and Lin, S., "Bestimmung des Kondensationsbeginns bei der Entspannung feuchter Luft in Überschalldüsen," *Forschung im Ingenieurwesen*, Vol. 33, No. 6, 1967, pp. 169–172.

[9]Zierep, J., "Ähnlichkeitsgesetze für Profilumströmungen mit Wärmezufuhr," *Acta Mechanica*, Vol. 1, No. 1, 1965, pp. 60–70.

[10]Zierep, J., *Similarity Laws and Modeling*, Gasdynamics Series of Monographs, edited by P. P. Wegener, Marcel Dekker, New York, 1971.

[11]Hall, R. M., "Onset of Condensation Effects as Detected by Total Pressure Probes in the Langley 0.3-Meter Transonic Cryogenic Tunnel,"

NASA TM 80072, May 1979.

[12]Hall, R. M., "Onset of Condensation Effects with an NACA 0012-64 Airfoil Tested in the Langley 0.3-Meter Transonic Cryogenic Tunnel," NASA TP 1385, April 1979.

[13]Kilgore, R. A., "Special Course on Advances in Cryogenic Wind Tunnel Technology," AGARD Rept. 774, von Kármán Inst., Rhode-Saint-Genèse, Belgium, June 1989.

[14]Wegener, P. P., "Nucleation of Nitrogen: Experiment and Theory," *Journal of Physical Chemistry,* Vol. 91, No. 10, 1987, pp. 2479–2481.

[15]Jordan, F. L., "Investigation at Near-Sonic Speed of Some Effects of Humidity on the Longitudinal Aerodynamic Characteristics of a NASA Supercritical Wing Research Airplane Model," NASA TM X-2618, Aug. 1972.

[16]Campbell, J. F., Chambers, J. R., and Rumsey, C. L., "Observation of Airplane Flow Fields by Natural Condensation," *Journal of Aircraft,* Vol. 26, No. 7, 1989, pp. 593–604.

[17]Robinson, C. E., Bauer, R. C., and Nichols, R. H., "Estimating Water Vapor Condensation Effects for Transonic and Supersonic Flow Fields," AIAA Paper 85-5020, Oct. 1985.

[18]Schnerr, G. H., and Dohrmann, U., "Transonic Flow Around Airfoils with Relaxation and Energy Supply by Homogeneous Condensation," *AIAA Journal,* Vol. 28, No. 7, 1990, pp. 1187–1193.

[19]Schnerr, G. H., and Dohrmann, U., "Numerical Investigation of Nitrogen Condensation in 2-D Transonic Flows in Cryogenic Wind Tunnels," *Proceedings of the IUTAM Symposium Adiabatic Waves in Liquid Vapor Systems,* edited by G. E. A. Meier and P. A. Thompson, Springer-Verlag, Berlin, 1990, pp. 171–180.

[20]Dohrmann, U., "Ein numerisches Verfahren zur Berechnung stationärer transsonischer Strömungen mit Energiezufuhr durch homogene Kondensation," Dissertation, Universität (TH) Karlsruhe, Fakultät für Maschinenbau, Karlsruhe, Germany, 1989.

[21]Moheban, M., and Young, J. B., "A Time-Marching Method for the Calculation of Blade to Blade Non-Equilibrium Wet Steam Flows in Turbine Cascades," Computational Methods for Turbomachinery, Paper C 76184, Birmingham, England, UK, 1984.

[22]Guha, A., and Young, J. B., "Stationary and Moving Normal Shock Waves in Wet Steam," *Proceedings of the IUTAM Symposium on Adiabatic Waves in Liquid Vapor Systems,* edited by G. E. A. Meier and P. A. Thompson, Springer-Verlag, Berlin, 1990, pp. 159–170.

[23]Young, J. B., and Guha, A., "Normal Shock-Wave Structure in Two-Phase Vapour-Droplet Flows," *Journal of Fluid Mechanics,* Vol. 228, July 1991, pp. 243–274.

[24]Ludwig, P. A., "Condensation of Water Vapor Makes F-14 Shock Waves Visible," *Aviation Week and Space Technology,* Nov. 1977, pp. 46, 47.

[25]Buckle, E. R., and Pouring, A. A., "Effects of Seeding on the Condensation of Atmospheric Moisture in Nozzles," *Nature,* Vol. 208, 1965, pp. 367–369.

[26]Schnerr, G. H., Bohning, R., Breitling, T., and Jantzen, H.-A., "Compressible Turbulent Boundary Layers with Heat Addition by Homogeneous Condensation," *AIAA Journal,* Vol. 30, No. 5, 1992, pp. 1284–1289.

[27]Schnerr, G. H., and Li, P., "Shock Wave Boundary Interaction with Heat Addition by Nonequilibrium Phase Transition," *International Journal of Multiphase Flow,* Vol. 19, No. 5, 1993, pp. 737–749.

[28]Thompson, P. A., "A Fundamental Derivative in Gasdynamics," *Physics of Fluids,* Vol. 14, No. 9, 1971, pp. 1843–1849.

[29]Cramer, M. S., "Nonclassical Dynamics of Classical Gases," *Nonlinear Waves in Real Fluids,* edited by A. Kluwick, Springer-Verlag, New York, 1991, pp. 91–145.

[30]Cramer, M. S., and Kluwick, A., "On the Propagation of Waves Exhibiting both Positive and Negative Nonlinearity," *Journal of Fluid Mechanics,* Vol. 142, May 1984, pp. 9–37.